

Ground Base Laser Torque Applied on LEO Satellites of Various Geometries

N. S. Khalifa*

*Mathematics Department, Hail University Deanship of Preparatory Year- Girls Branch, Hail, KSA
National Research Institute of Astronomy and Geophysics (NRIAG), Cairo, Egypt*

Abstract

This paper is devoted to investigate the feasibility of using a medium power ground-based laser to produce a torque on LEO satellites of various shapes. The laser intensity delivered to a satellite is calculated using a simple model of laser propagation in which a standard atmospheric condition and linear atmospheric interaction mechanism is assumed. The laser force is formulated using a geocentric equatorial system in which the Earth is an oblate spheroid. The torque is formulated for a cylindrical satellite, spherical satellites and for satellites of complex shape. The torque algorithm is implemented for some sun synchronous low Earth orbit cubesats. Based on satellites perigee height, the results demonstrate that laser torque affecting on a cubesat has a maximum value in the order of 10^{-9} which is comparable with that of solar radiation. However, it has a minimum value in the order of 10^{-10} which is comparable with that of gravity gradient. Moreover, the results clarify the dependency of the laser torque on the orbital eccentricity. As the orbit becomes more circular it will experience less torque. So, we can conclude that the ground based laser torque has a significant contribution on the low Earth orbit cubesats. It can be adjusted to obtain the required control torque and it can be used as an active attitude control system for cubesats.

Key words: linear atmospheric mechanism of laser interactions, radiation torque, The Attitude Determination and Control System (ADCS), geocentric equatorial coordinate systems, spherical and cylindrical coordinate systems, LEO satellites and cubesats.

1. Introduction

The Attitude Determination and Control System (ADCS) is to stabilize the spacecraft against attitude disturbing influences resulting from the environment in the Earth's orbit in order to orient it in the desired fixed pointing. Active control of the attitude of a satellite can be achieved by a number of different actuators: reaction wheels, thrusters, control moment gyroscopes or magnetic torquers. However, the magnetic torquers are widely used actuators for geostationary satellites, small satellites, and microsatellites. These high-tech devices interact with the Earth's magnetic field and create a control torque, which can be adjusted to the required value. Combined with one or more reaction wheels, they provide all the control you need to maintain

your spacecraft's attitude [8] and [14].

Unlike thrusters, magnetorquers are lightweight, reliable, and energy-efficient. A further advantage over momentum wheels and control moment gyroscopes is the absence of moving parts and therefore significantly higher reliability. However, they require a thoughtful design and careful assembly.

The main disadvantage of magnetorquers is that the strength of the magnets should be chosen to be strong enough to overcome the greatest expected disturbances (as given in table 1). A broader disadvantage is the dependence on Earth's magnetic field strength, making this approach unsuitable for deep space missions, and also more suitable for low Earth orbits as opposed to higher ones like the geosynchronous. The dependence on the highly variable intensity of Earth's

This is an Open Access article distributed under the terms of the Creative Commons Attribution Non-Commercial License (<http://creativecommons.org/licenses/by-nc/3.0/>) which permits unrestricted non-commercial use, distribution, and reproduction in any medium, provided the original work is properly cited.

© * Assistance professor, Corresponding author, E-mail: asmaa_2000_2000@yahoo.com

magnetic field is also problematic since the attitude control problem becomes highly nonlinear. It is also impossible to control attitude in all three axes even if the full three coils are used, since torque can only be generated perpendicular to the Earth's magnetic field vector [11] and [13].

The main issue of this work is to investigate the feasibility of using a medium power (5kw) to produce a torque on low Earth orbit cubesats in order to overcome some disadvantages of the traditional attitude actuators. The use of a ground based laser to produce a perturbing force goes back to the study of laser orbital perturbations by some scientists. The use of this medium power has the advantage of being inexpensive, and suffering a less amount of atmospheric attenuation. Moreover, it is safe in use where it cannot damage the satellite surface [3], [10] and [6].

Table 1. Worst-case expected disturbance torques for a 1-U CubeSat at 700 km [11]

The source	Torque (Nm)
Aerodynamics	8.7×10^{-10}
Gravity gradient	6.8×10^{-10}
Solar pressure	3.8×10^{-9}
Residual Magnetic Moment	4.5×10^{-7}
Total	4.6×10^{-7}

2. Laser Torque Model.

2.1 Laser Intensity.

The laser intensity delivered to the satellite surface is determined using an analytical model of long range laser beam propagation through the atmosphere. For standard atmospheric conditions, this model considers only the linear mechanism of laser atmospheric interactions. Moreover, the atmospheric turbulences are countered by using the adaptive optics and technical capabilities of the laser system. Based on that model, the laser intensity is proportional to the laser power and inversely proportional to satellite altitude and laser divergence. The laser intensity is given by [2] and [10]:

$$S(\rho) = \frac{P}{\pi u^2 \theta^2} \text{Exp} - \left[\left[\frac{\sigma_{scat}^{mol}(0)h}{\sin(\phi)} \right] \left[1 - \text{Exp} \left(-\frac{\rho \sin(\phi)}{h} \right) \right] + \sigma_{scat}^{aer}(\rho) \right] \quad (1)$$

where, u is the satellite altitude, P is the laser power, θ is the laser divergence, ϕ is the elevation angle, $\sigma_{scat}^{mol}(0)$ is the molecule scattering coefficient at sea level, σ_{scat}^{aer} is the aerosols scattering coefficient and h is the sea level altitude.

2.2 The laser force.

The total radiant force exerted on a flat non-perfectly reflecting surface is given by [9]:

$$\vec{f} = \frac{SA}{C} \psi \hat{m} \quad (2)$$

where,

$$\psi = \left[4\rho'\beta \cos^4 \eta + 2(1+\rho'\beta)(B_f \rho'(1-\beta) + \alpha' \frac{\epsilon_f B_f - \epsilon_b B_b}{\epsilon_f + \epsilon_b}) \cos^3 \eta + \left\{ (B_f \rho'(1-\beta) + \alpha' \frac{\epsilon_f B_f - \epsilon_b B_b}{\epsilon_f + \epsilon_b})^2 + (1-\rho'\beta)^2 \right\} \cos^2 \eta \right]^{1/2} \quad (3)$$

where \hat{m} is a unit vector directed through the force direction, c is the speed of light and S is the radiation irradiance at the debris surface, η is the radiation incident angle to the debris surface normal, β is the debris surface specularity, ρ' is the debris surface reflectivity, B_f and B_b are the non-Lambertian coefficient of the front and back surfaces of the spacecraft, respectively, α' is the spacecraft absorption coefficient, and ϵ_f and ϵ_b are the front and back debris surface emissivity, respectively.

For non-perfectly reflecting surfaces, The force vector, \hat{m} , is not directed normal to the surface. But, it inclines by an angle \mathcal{G} , known as the cone angle, to the incident direction, \hat{u} , as depicted in figure 1. So, the force components in the incident direction will be:

$$\vec{f}_u = \frac{SA}{C} \psi \cos \mathcal{G} \hat{u} \quad (4)$$

2.3 The coordinate systems.

The geocentric equatorial system is used with the unit vectors; \hat{e}_x directed parallel to the Earth equatorial plane, \hat{e}_y directed in the plane that contains the meridian of the sub-satellite point and \hat{e}_z directed normal to the equatorial plane. As shown in Fig. 1, the incident radiation vector, $\vec{\rho}$, is given by:

$$\vec{u} = \vec{r} - \vec{r}_E, \quad (5)$$

where \vec{r} is the satellite position vector and \vec{r}_E is the Earth radius vector (station coordinates). For an oblate Earth, the Earth radius vector is given by [4]:

$$\vec{r}_E = \begin{pmatrix} G_1 \cos \varphi_g \cos \theta \\ G_1 \cos \varphi_g \sin \theta \\ G_2 \sin \varphi_g \end{pmatrix}, \quad (6)$$

with

$$G_1 = \frac{a_e}{(1 - (2f'_e - f_e'^2) \sin^2 \varphi_g)^{1/2}} + h \tag{7}$$

$$G_2 = \frac{a_e(1 - f_e'^2)}{(1 - (2f'_e - f_e'^2) \sin^2 \varphi_g)^{1/2}} + h$$

where a_e is the Earth's Equatorial radius, f'_e is the Earth's flattening, φ_g is the geodetic latitude, h is the height above sea level and θ is the sidereal time.

The satellite position vector, \bar{r} , in the geocentric coordinate system, is given by [4]:

$$\bar{r} = r \begin{pmatrix} \cos \Omega \cos(\omega + \nu) - \sin \Omega \sin(\omega + \nu) \cos i \\ \sin \Omega \cos(\omega + \nu) + \cos \Omega \sin(\omega + \nu) \cos i \\ \sin(\omega + \nu) \sin i \end{pmatrix}, \tag{8}$$

with

$$r = \frac{a(1 - e^2)}{1 + e \cos \nu},$$

where Ω is the longitude of the ascending node, ω is the argument of perigee, ν is the true anomaly, i the inclination, a is the semi-major axis and e is the eccentricity. Using the geocentric coordinate system, the incident radiation vector is:

$$\bar{u} = u_x \hat{e}_x + u_y \hat{e}_y + u_z \hat{e}_z \tag{9}$$

with

$$u_x = r(\cos \Omega \cos(\omega + \nu) - \sin \Omega \sin(\omega + \nu) \cos i) - G_1 \cos \varphi_g \cos \theta, \tag{10}$$

$$u_y = r(\sin \Omega \cos(\omega + \nu) + \cos \Omega \sin(\omega + \nu) \cos i) - G_1 \cos \varphi_g \sin \theta, \tag{11}$$

$$u_z = r \sin(\omega + \nu) \sin i - G_2 \sin \varphi_g. \tag{12}$$

2.4 The Laser Torque

The radiation torque, \hat{N} , acting on a spacecraft is given by

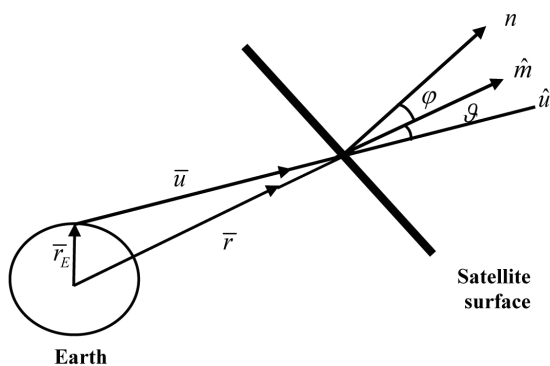


Fig. 1. The laser intensity delivered to the satellite surface

the general expression [1], [14] and [15]:

$$\bar{N} = \int \bar{R} \times d\bar{f}, \tag{13}$$

where \bar{R} is the vector from the spacecraft's center of mass to the element of the satellite projected area dA . The geocentric components of laser torque, \hat{N} , acting on a spacecraft is given by:

$$N_x = \frac{SA}{C} \psi \cos \vartheta \int (R_y u_z - R_z u_y) dA \tag{14}$$

$$N_y = \frac{SA}{C} \psi \cos \vartheta \int (R_z u_x - R_x u_z) dA \tag{15}$$

$$N_z = \frac{SA}{C} \psi \cos \vartheta \int (R_x u_y - R_y u_x) dA \tag{16}$$

For a high laser repetition rate, many laser shots fire toward the satellite over an interval of time each one of intensity S . Consequently, the laser force can be considered as a continuous function. Thus, the total laser torque over an interval of time, $I=t_1-t_0$, can be written as:

$$\bar{N}_I = \int_{t=t_0}^{t=t_1} \bar{N} dt, \tag{17}$$

where t_0 is the time of the starting laser firing and t_1 is the time of its stopping.

In order to evaluate the previous integrals, the vector \bar{R} must be determined. So, satellite geometry must be considered. In the next sections, three particular cases; circular cylindrical satellite, spherical satellite and satellite of complex shape will be studied.

2.5 Laser Torque Applied on Circular Cylindrical Satellite.

The position vector of the surface elements can be expressed in terms of a coordinate system with unit vectors \hat{e}_x , \hat{e}_y and \hat{e}_z , where its origin ($\hat{e}_x=0$, $\hat{e}_y=0$ and $\hat{e}_z=0$) is at the geometric center of the satellite, as follows:

$$\bar{R} = \rho \cos \phi \hat{e}_x + \rho \sin \phi \hat{e}_y + z \hat{e}_z$$

where ρ is the radius of the circular base and ϕ is the azimuthal angle. The position vector, \bar{R} , can be transformed into the following geocentric coordinate:

$$\bar{R} = R_x \hat{e}_x + R_y \hat{e}_y + R_z \hat{e}_z$$

with

$$R_x = \rho \cos \phi + r(\cos \Omega \cos(\omega + \nu) - \sin \Omega \sin(\omega + \nu) \cos i) \tag{18}$$

$$R_y = \rho \sin \phi + r(\sin \Omega \cos(\omega + \upsilon) + \cos \Omega \sin(\omega + \upsilon) \cos i) \quad (19)$$

$$R_z = z + r \sin(\omega + \upsilon) \sin i \quad (20)$$

The illuminated surfaces of the cylinder satellite are a circular flat surface of radius ρ and an area $A_1 = \pi \rho^2$ in addition to a portion σ of the cylinder side of height H approximated and an area, $A_2 = 2\sigma \pi \rho H$, as in fig. 2.

Substituting into eqs. (14-16) and integrating over the areas A_1 and A_2 , laser torque applied on a cylindrical satellite is obtained.

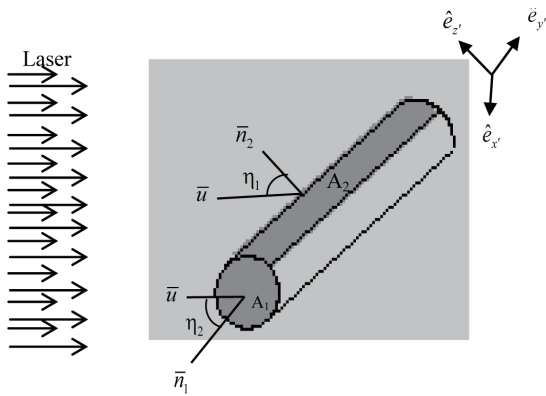


Fig. 2. The illuminated surfaces of the circular cylindrical satellite

2.6 Laser Torque Applied on Spherical Satellite.

The position vector of the surface elements can be expressed in terms of a coordinate system with unit vectors \hat{e}_x, \hat{e}_y and \hat{e}_z , where its origin ($\hat{e}_x=0, \hat{e}_y=0$ and $\hat{e}_z=0$) is at the geometric center of the satellite, as follows:

$$\hat{R} = \rho \cos \vartheta \sin \phi \hat{e}_x + \rho \sin \phi \sin \vartheta \hat{e}_y + \rho \cos \phi \hat{e}_z$$

where ρ is the radius of the sphere, ϑ is the polar angle and ϕ is the azimuthal angle. The position vector, \hat{R} , can be transformed into the following geocentric coordinate:

$$\bar{R} = R_x \hat{e}_x + R_y \hat{e}_y + R_z \hat{e}_z$$

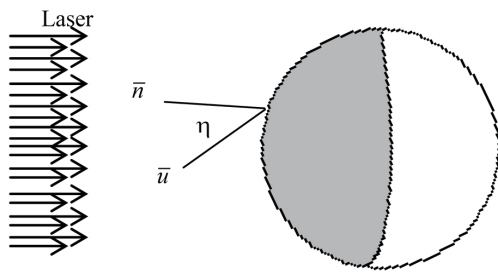


Fig. 3. The illuminated surfaces of the spherical satellite

with

$$R_x = \rho \cos \vartheta \sin \phi + r(\cos \Omega \cos(\omega + \upsilon) - \sin \Omega \sin(\omega + \upsilon) \cos i) \quad (21)$$

$$R_y = \rho \sin \phi \sin \vartheta + r(\sin \Omega \cos(\omega + \upsilon) + \cos \Omega \sin(\omega + \upsilon) \cos i) \quad (22)$$

$$R_z = \rho \cos \phi + r \sin(\omega + \upsilon) \sin i \quad (23)$$

The illuminated surfaces of the spherical satellite can be considered as a hemisphere with an area $A = 2\pi \rho^2$, as shown in fig. 3.

Substituting into eqs. (14-16) and integrating over the area A , the laser torque applied on a spherical satellite is obtained.

2.7 Laser Torque Applied on Satellite of complex shape.

In order to compute the torque applied on spacecraft of complex shape, we can follow the following scheme [5] and [7]:

- 1-Approximate each surface by means of simple geometric shapes (planes, cylinders, cones, spheres,..., etc.).
- 2-Determined the torque applied on each surface independently.
- 3-Then, the total torque applied over the whole spacecraft is obtained by the vector sum of all torques applied on each elementary surface.

3. Numerical Application.

Based on the standard atmospheric conditions and taking into consideration that $\sigma_{scat}^{mol}(0) = 1.7 \times 10^{-2} km^{-1}$ and $\sigma_{scat}^{aer} = .1 km^{-1}$ [12]. In case of clear weather conditions, the propagation of a medium-powered 5 kW ground-based laser with a divergence of .1 mrad is illustrated in the following figure:

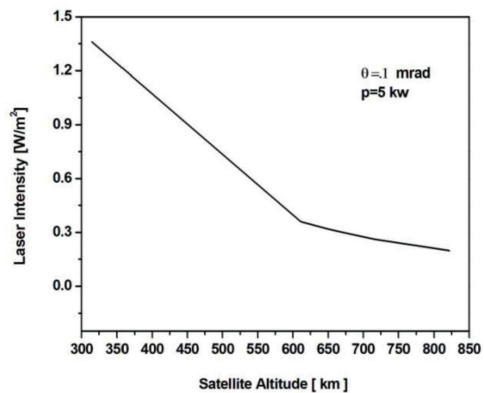


Fig. 4. laser intensity delivered to LEO satellites of different altitudes

As illustrated in fig 4, the laser intensity has a significant dependency on the altitude. It has a maximum value $\sim 1.4W/m^2$ at the altitude of 314.4 km. However, it has a minimum value $\sim 0.2W/m^2$ at an altitude of 823 km.

In the present work, the laser torque applied is calculated under the following postulates:

1-The laser source is located in the Helwan SLR station in Egypt with latitude of 29.86° N, longitude of 31.34° E and elevation of 145.46 m.

2-The radiation falls normal to the satellite surface (i.e. $\eta = 0$) and the satellite projected area is half of the total area.

3-The satellite surface is made of Aluminium, so it can be considered as a perfectly reflecting surface. Therefore, the laser force will be duplicated, where the satellite surface specularity $\beta=1$ and the satellite surface reflectivity $\rho'=1$. While the spacecraft absorption coefficient $\alpha'=0$.

Based on the previous postulates and for a given time, the torque produced by a 5 kw laser beam is calculated for some

low Earth orbit cubesats and the results are illustrated in the following table:

As illustrated in table 2, the satellites are arranged in ascending order according to their perigee height as it is clear in the table that the laser torque depends on the latitude, since the radiation force is inversely depended on the satellite altitude. The laser torque has a maximum value in the order of for a cubesat with a perigee height close to 600 km, however, it has a minimum value in the order for a cubesat perigee height close to 800 km.

In addition to the satellite height, the dependency of the ground based laser torque on the orbital eccentricity is studied and illustrated in table (3).

As illustrated in table 3, the satellites are chosen to be nearly of the same altitude and inclination and they are arranged in descending order according to their eccentricity as it clear in the table that the laser torque directly depends on the orbital eccentricity.

Table 2. laser torque affecting on LEO cubesats at different altitudes using 5 kw laser beam at a given time.

Satellite	NORD ID	Perigee height[km]	Eccentricity	Inclination [Degree]	Laser Torque [N m]
DELFI C3	32789	605.4	0.01364	97.7971	1.05×10^{-9}
AAUSAT CUBESAT 2	32788	611.1	0.013174	97.7842	1.06×10^{-9}
COMPASS 1	32787	612	0.014275	97.7836	1.08×10^{-9}
SEEDS	32791	613.8	0.014336	97.7823	1.07×10^{-9}
CANX-2	32790	616.2	0.014593	97.7806	1.07×10^{-9}
CUTE-1.7+APD II	32785	616.6	0.013592	97.7815	1.06×10^{-9}
CAPE 1	31130	650.3	0.010201	97.8851	1.68×10^{-9}
CP3	31129	650.3	0.069872	97.843	1.45×10^{-9}
LIBERTAD 1	31128	650.9	0.010211	97.8842	1.69×10^{-9}
CSTB 1	31122	651.9	0.084558	97.8666	1.47×10^{-9}
MAST	31126	652.1	0.094379	97.8753	1.52×10^{-9}
SAUDICOMSAT 6	31121	655.1	0.078933	97.8519	1.44×10^{-9}
SAUDICOMSAT 4	31127	656.1	0.069872	97.843	1.41×10^{-9}
SAUDICOMSAT 7	31119	657.4	0.061068	97.8357	1.37×10^{-9}
SAUDICOMSAT 5	31124	658.2	0.052042	97.8323	1.32×10^{-9}
SAUDICOMSAT 3	31125	659.1	0.043911	97.8331	1.27×10^{-9}
EGYPTSAT1	31117	662.2	0.04541	97.8774	8.97×10^{-10}
SAUDISAT 3	31118	663.5	0.014059	97.854	9.64×10^{-10}
SSETI-EXPRESS DEB	28897	684.0	0.09334	98.7127	1.56×10^{-9}
CUBESAT XI-V	28895	684.6	0.018889	97.893	1.56×10^{-9}
UWE-1	28892	684.8	0.018433	97.889	1.55×10^{-9}
BEESAT	35933	714.8	0.07454	98.3482	2.88×10^{-10}
UWE-2	35934	715.9	0.06907	98.3437	2.66×10^{-10}
ITUPSAT1	38079	716.6	0.08961	98.3531	2.66×10^{-10}
SWISSCUBE	35932	716.7	0.09084	98.3457	2.59×10^{-10}
AAU CUBESAT	27844	820.8	0.09308	98.6961	8.84×10^{-10}
CANX-1	27847	820.9	0.09653	98.6944	8.83×10^{-10}
CUTE-1	27845	821.5	0.09592	98.7036	8.95×10^{-10}
CUBESAT XI-IV	27848	822.5	0.018889	97.893	9.01×10^{-10}
QUAKESAT	27846	823.3	0.08377	98.715	8.77×10^{-10}
DTUSAT	27842	834.5	0.0934	98.6959	8.45×10^{-10}

Table 3. Dependency of the laser torque on satellite eccentricity

Satellite	NORD ID	Eccentricity	Laser Torque[N m]
MAST	31126	0.094379	1.52×10^{-9}
CSTB 1	31122	0.084558	1.47×10^{-9}
SAUDICOMSAT 6	31121	0.078933	1.44×10^{-9}
SAUDICOMSAT 4	31127	0.069872	1.41×10^{-9}
SAUDICOMSAT 7	31119	0.061068	1.37×10^{-9}
SAUDICOMSAT 5	31124	0.052042	1.32×10^{-9}
SAUDICOMSAT 3	31125	0.043911	1.27×10^{-9}
COMPASS 1	32787	0.014275	1.08×10^{-9}
AAUSAT CUBESAT 2	32788	0.013174	1.06×10^{-9}
SWISSCUBE	35932	0.09084	2.59×10^{-10}
ITUPSAT1	38079	0.08961	2.66×10^{-10}
BEESAT	35933	0.07454	2.88×10^{-10}
UWE-2	35934	0.06907	2.66×10^{-10}

4. Conclusion

A simple model of radiation torque affecting on satellites of various shapes is formulated using the geocentric equatorial coordinate system. Based on the model, the intensity delivered to the target is proportional to the laser power and inversely proportional to the beam divergence as given by eq. 1. So, we can adjust the laser power and divergence (by choosing the beam wavelength) in order to obtain the required control torque.

The current numerical test confirms that the laser torque has significant contribution on the low Earth orbit cubesats. The results show that the laser torque has a maximum value in the order of 10^{-9} which is comparable with that of solar radiation. However, it has a minimum value in the order of 10^{-10} which is comparable with that of the gravity gradient. Moreover, the laser torque depends directly on the orbital eccentricity whereas when the orbit becomes more circular it will experience less torque. Therefore, we can conclude that the laser torque can be used as an active attitude control system for cubesats.

Acknowledgement

The author is indebted for the helpful discussions and comments of Prof. Kh. I. Khalil and Prof. El-Saftawy, M.I .

References

- [1] Beletskii, V. V, "motion of an artificial satellite about its center of mass", NASA translation, NASA TF - 429, 1966.
 [2] El-Saftawy, M. I., Afaf, M. A. E., and Khalifa, N.S.,

"Analytical Studies of Laser Beam Propagation through the Atmosphere", *Proceeding of 6th International Conference on Laser Science and Applications(ICLAS-07)*, Cairo, Egypt, 2007.

[3] El-saftawy, M.I., and Makram, I. "The laser shots as a perturbing force on spacecraft's orbit", *NRIAG Journal of Astronomy And Astrophysics*. Vol. 5, No. 1, 2004, pp. 00-00.

[4] Escobal, P.R., *Methods of Orbit Determination*, John Wiley and Sons, Inc., New York, London, Sydney, 1965.

[5] Harris, M. and Lyle, R., "Spacecraft Radiation Torque", NASA Space Vehicle Design Criteria (Guidance and Control) NASA SP-8027, October 1969.

[6] James Mason, Jan Stupl , William Marshall, and Creon Levit, "Orbital Debris-Debris Collision Avoidance", *Journal of Advances in Space Research*, Vol. 48, No. 10, 2011, pp. 1643-1655.

[7] Ping, J., Sengoku, A., Nagaoka, N., Iwata, T., Matsumoto, K., and Kawano, N., "How solar radiation pressure acts on RSAT and VSAT with a small evolving tip-off in SELENE", *Earth Planets Space*, Vol.53, 2001, pp. 919-925.

[8] Karla Patricia Vega, "Attitude Control System for CubeSat for Ions, Neutrals, Electrons and MAGnetic Field (CINEMA)", M.S. Thesis, Graduate Division of Engineering and Mechanical Engineering, University of California, Berkeley, 2009.

[9] Colin Robert McInnes, *Solar Sailing: Technology, Dynamics and Mission Applications*, Springer-Praxis Series in Space Science and Technology, Chichester, 1999.

[10] N.S. khalifa, "Effect of an Artificial Radiant Force on the Spacecraft's Orbit", Ph. D. Thesis, Department Astronomy and Meteorology, Cairo university, 2009.

[11] Rawashdeh, S., "PASSIVE ATTITUDE STABILIZATION

FOR SMALL SATELLITES”, M.S. Thesis, College of Engineering, University of Kentucky, Kentucky, 2009.

[12] Oleg F. Prilutsky, M.N. Fomenkova, “Laser beam scattering in the atmosphere”, *Science & Global Security*, Vol. 2, No.1, 1990, pp79-86.

[13] Francois-Lavet, V., “Study of passive and active attitude control systems for the OUFIT nanosatellites”, M.S.

Thesis, Faculty of Applied Sciences, University of Liège, 2010.

[14] James R Wertz ,”*Spacecraft Attitude Determination and Control*, D. Reidel, Dordrecht, Holland, 1978.

[15] Zanardi M.C and Vilhena de Moraes, “ABC Analytical and semi-analytical analysis of an artificial satellite's rotational motion”, *Celestial Mechanics and Dynamical Astronomy*, Vol. 75, No. 4, 1999, pp. 227-250.